

COMMENTARY

Extrapolation of microearthquake populations to predict consequences of low-probability high impact events: the Pohang case study revisited

Rob Westaway¹

¹James Watt School of Engineering, University of Glasgow, James Watt (South) Building, Glasgow G12 8QQ, UK.

Corresponding author: Rob Westaway (robert.westaway@gla.ac.uk)

Key Points:

- The Pohang EGS project in Korea is the first to have caused an induced earthquake as large as M_w 5.5, with fatal consequences.
- The previously-reported low b-value of the earthquakes from the well stimulation is an artefact of a mixed set of magnitude determinations
- Proper calibration and transparent reporting of such datasets is essential; their results might influence criminal trials of EGS developers

Abstract

The November 2017 magnitude (M_W) 5.5 Pohang, Korea, earthquake, induced by an Engineered Geothermal Systems (EGS) project, caused one fatality and ~US\$300M of economic consequences. It has been proposed that a significant probability of such losses was predictable beforehand, from the small earthquakes caused by well-stimulation, so the project should have been suspended, implying that its developer was remiss for not doing so. This argument depends on the low (~0.61) estimated b-value of this earthquake population. However, it is shown that many of the magnitude determinations are inaccurate (underestimated) and the true b-value is higher (1.12 for one subset). The probability of any earthquake as large as $M_W=5.5$, predicted beforehand by extrapolation, was thus much lower than has been claimed. This analysis highlights the necessity of taking care over accuracy when reporting datasets like this, especially in situations where such analyses might influence criminal trials of EGS developers.

Plain Language Summary

The continuing development of geo-engineering technologies involving fluid injection into, or production from, the subsurface, requires robust procedures for establishing liability for consequences of large anthropogenic earthquakes. Scientific outputs that may contribute to such assessments, and might indeed feature in legal actions against developers who are held responsible, include magnitudes of populations of small earthquakes. It is therefore essential to ensure that such outputs are accurate.

1 Introduction

The Pohang EGS project has been thoroughly described (e.g., Lee et al., 2011; Yoon et al., 2015; Grigoli et al., 2018; Kim et al., 2018; Ellsworth et al., 2019; Hofmann et al., 2019; Lee et al., 2019). In summary, well PX-1 was initially drilled vertically, then side-tracked ~600m WNW at ~4.2km depth. Vertical well PX-2 reaches a similar depth; in November 2015, during its drilling, mud-loss, accompanied by small earthquakes, occurred into what proved to be the seismogenic fault of the November 2017 $M_W=5.5$ earthquake, named the Namsong Fault. However, this 2015 seismicity, which indicated that this fault was critically-stressed, went unrecognized, the temporary seismograph network around the EGS site being not yet operational. This seismicity was recognized later (Kim et al., 2018) when archived data from station PHA2, ~10km north of the site, were examined. PHA2 is part of a network of permanent stations operated by the Korea Meteorological Administration (KMA) to monitor regional seismicity. KMA determines magnitudes (designated here as M_K) using a non-standard procedure, routinely reporting events with $M_K \geq 2.0$. Five stimulations took place to create a hydraulic connection through the granite between the wells: in PX-2 in February 2016, April 2017, and September 2017; and in PX-1 in December 2016 and August 2017. This EGS project was implemented by Korean organizations led by the Pohang Geothermal Power Co., a subsidiary of NexGeo Inc. (www.nexgeo.com), who were responsible for all activities. My involvement arose because the August 2017 stimulation was part of project DESTRESS, funded by the European Commission Horizon 2020 programme.

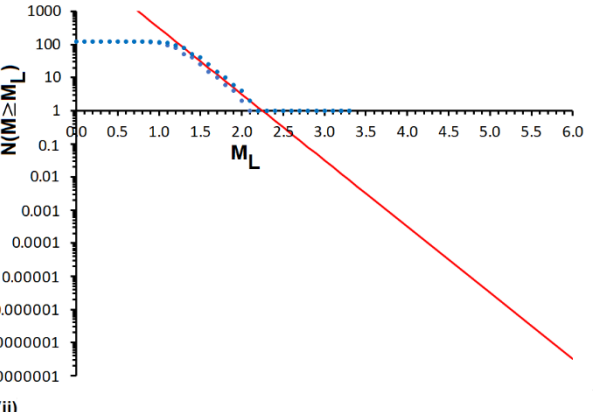
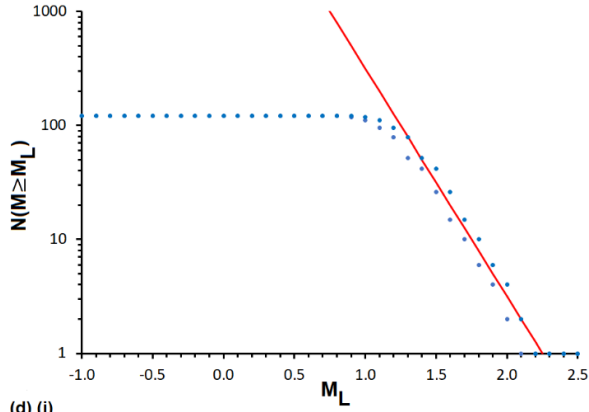
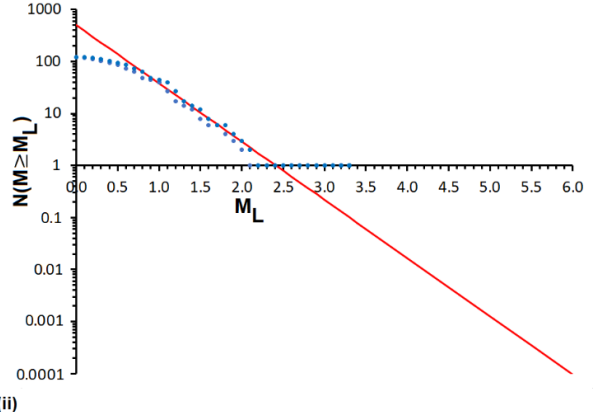
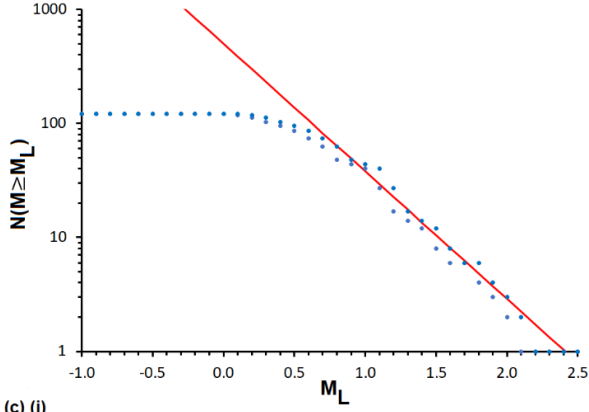
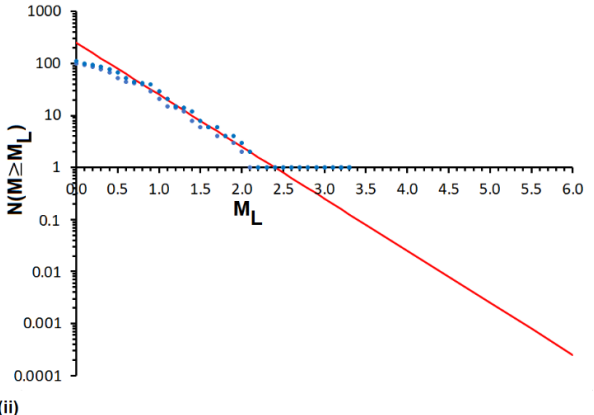
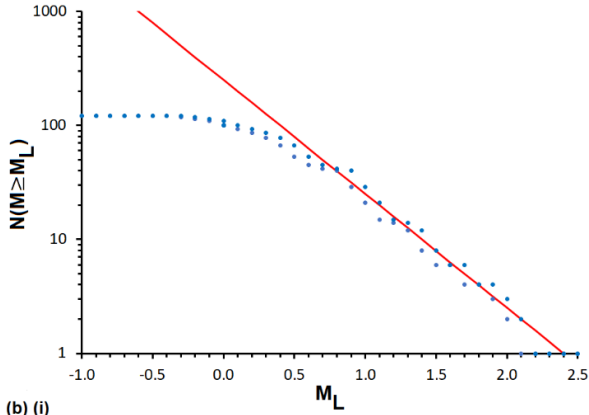
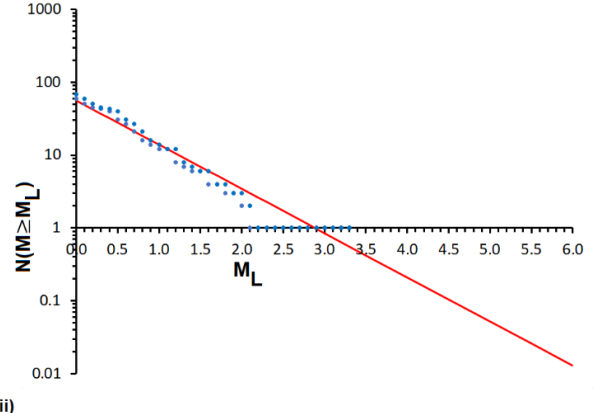
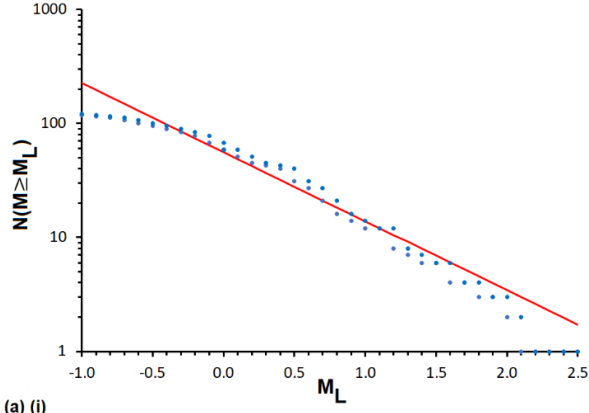


Figure 1. Earthquake populations caused by stimulation of Pohang well PX-2 and Gutenberg-Richter law fits. **(a)** As reported by Langenbruch et al. (2020), with $a=1.75$ and $b=0.607$. **(b-d)** Potential revisions for $M_{LT}=M_{LO}=2$: **(b)** For $K=1/\log_{10}(20)\approx 0.769$; $a=2.4$ and $b=1$; **(c)** For $K=0.64$; $a=2.7$ and $b=1.12$; **(d)** For $K=0.36$; $a=4.5$ and $b=2$.

The Korean government appointed a commission to investigate if this EGS project caused the $M_W=5.5$ earthquake, NexGeo being thereby required to disclose project data. These data, plus other evidence including from station PHA2, informed the commission report (Kim et al., 2019); commission members have also used this dataset in publications (e.g., Ellsworth et al., 2019; Woo et al., 2019; Langenbruch et al., 2020). In contrast, much of this dataset was unavailable to DESTRESS participants, who have nonetheless developed much of the current understanding of this earthquake, notably for aspects unexplored by the commission (e.g., Grigoli et al., 2018; Hofmann et al., 2019; Westaway and Burnside, 2019; Westaway et al., 2020). The impression thus created, of commission ‘earthquake detectives’ exposing blunders by bumbling project participants (e.g., Baraniuk, 2019), is not the whole story. The probable cause of the $M_W=5.5$ earthquake was the effect of injected surface water entering the Namsong Fault and dissolving minerals, bringing it closer to the condition for slip (e.g., Westaway and Burnside, 2019; Westaway et al., 2020), a mechanism unrelated to the small events during the stimulations.

Probabilities P of large-magnitude earthquakes can be predicted by extrapolation of the ‘tails’ of small-event populations (e.g., Smith, 1981). Numbers, N , in any population are expected to follow the Gutenberg-Richter law $N(M\geq M_W)=10^a\times 10^{-b\times M}$, where a and b are constants. Langenbruch et al. (2020) propose very low b -values for the Pohang well-stimulation dataset: 0.607 ± 0.068 for PX-2 (Fig. 1(a)(i)); 0.762 ± 0.127 for the smaller PX-1 population. For the PX-2 population, this implies estimates, ahead of the $M_W=5.5$ earthquake, of $P\sim 5\%$ and $\sim 1\%$ for magnitude ≥ 5.0 and ≥ 6.0 events (Fig. 1(a)(ii)). Langenbruch et al. (2020) have integrated such extrapolation with a model for probabilistic calculations of earthquake-damage. They concluded that as early as the February 2016 PX-2 stimulation the EGS developers might thus have identified a significant risk (e.g., $P\sim 1\%$ for magnitude ≥ 5.0), even though the largest earthquake by then had M_W only ~ 1.6 (Woo et al., 2019). However, this conclusion depends critically on the low b -value. Induced earthquake-populations instead typically have $b>1$ (e.g., for ten populations considered by Dempsey et al., 2016, b spanned 1.1-2.0 with a ~ 1.4 median), casting doubt on the Langenbruch et al. (2020) analysis.

My role in the August 2017 PX-1 stimulation was to determine M_W values to implement the ‘traffic light’ protocol. To facilitate this, the local station network was supplemented by a geophone-chain in well PX-2 (Hofmann et al., 2019). A processing workstation had been established, using InSite software (Itasca Consulting Ltd., Shrewsbury, England) but, although events caused by the first three stimulations had been located, no magnitudes had been determined; the software had rejected the amplitudes of imported seismograms as implausible, because of incorrect calibrations (conflating digital counts and volts). Thus, at this time the only magnitudes available were those reported by KMA for $M_K\geq 2.0$ events: at 20:31 on December 22, 2016 (M_K 2.2), 12:32 on December 29, 2016 (M_K 2.2), and 02:31 and 08:16 on April 15, 2017 (M_K 3.1 and 2.0), insufficient to determine a b -value.

The August 2017 ‘traffic light’ protocol required actions at $M_W \geq 1.0$, ≥ 1.4 , ≥ 1.7 and ≥ 2.0 (Hofmann et al., 2019). Signal amplitudes at one local surface station, MSS-01 (~1.8km north of the site), initiated alerts. Data were then processed to determine hypocenters, focal mechanisms, and seismic moment M_O , then M_W after Hanks and Kanamori (1979). Along with smaller earthquakes, this procedure determined $M_W=1.4$ and 1.8 for events at 04:58 and 21:42 on August 13, 2017. The latter event triggered a ‘red’ traffic-light action, ending injection and initiating flowback. Re-analysis of this dataset for the Hofmann et al. (2019) publication provided M_W -values for 52 events. It yielded M_W 1.20 and 1.93, rather than 1.4 and 1.8, for the events that influenced the stimulation, this high consistency arising because both analyses applied standard procedures in a valid manner. The Hofmann et al. (2019) earthquake population has $b=1.12$ (Fig. 2(a)), well above the 0.76 reported by Langenbruch et al. (2020) for PX-1 stimulations. In contrast, for the 21:42 event, Kim et al. (2019) and Woo et al. (2019) reported $M_W=1.21$ along with local magnitude $M_L=0.67$, Langenbruch et al. (2020) also reporting $M_L=0.67$. Such discrepancies require resolution before any resulting b -values are considered reliable.

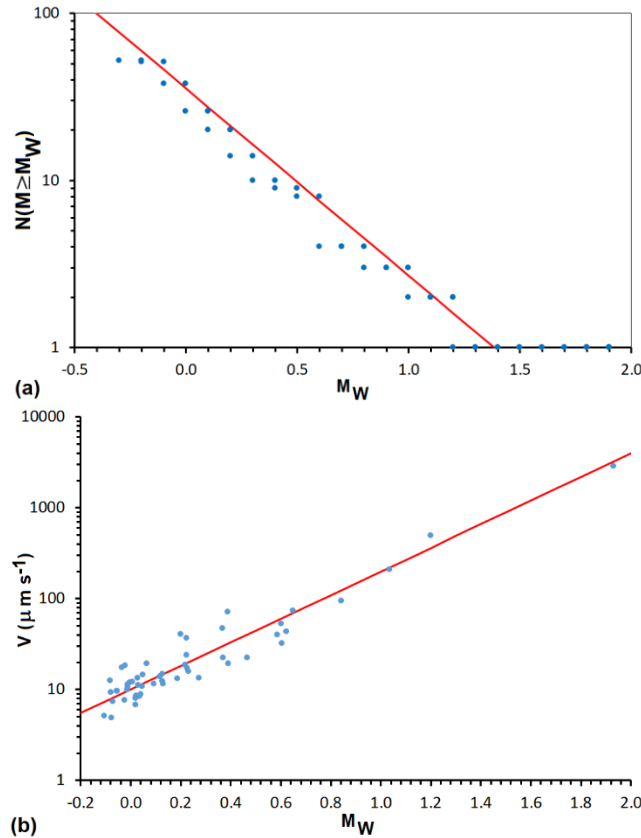


Figure 2. The earthquake population associated with the August 2017 stimulation of Pohang well PX-1, as reported by Hofmann et al. (2019). (a) Gutenberg-Richter law fit for $a=1.55$ and $b=1.12$. (b) Peak ground velocity V in $\mu m s^{-1}$ at seismograph station MSS-01 versus M_W for the earthquakes in (a), including line of best fit for $V=C \times M_W^D$ with $C=10$ and $D=1.3$, for which a unit increase in M_W correlates with a ~20-fold increase in V .

2 Reconciling magnitude and b-value determinations for Pohang earthquakes

Key to reconciling such discrepancies, it is suggested, are the different sampling intervals of the various stations. The Pohang local network and downhole geophone chain recorded every 1ms, the instruments at PHA2 every 10ms. Both sets of records were digitally filtered to remove signal above the Nyquist frequency f_N , >50 or $>500\text{Hz}$, respectively. From standard theory (Eshelby, 1957), $M_0 = (16/7) \times \Delta\sigma \times a^3$ with $\Delta\sigma$ the coseismic stress drop and a the radius of the earthquake source. This formula assumes the ratio of seismic velocities $V_P/V_S = \sqrt{3}$ (i.e., Poisson's ratio 0.25); formulas for more general rock properties are available (e.g., Westaway and Younger, 2014). Many workers have modelled earthquake sources with flat displacement spectra below a corner frequency f_C , above which spectral displacement tails off (e.g., Brune, 1970; Sato and Hirasawa, 1973; Madariaga, 1976; Kaneko and Shearer, 2014; Madariaga and Ruiz, 2016). In general, $f_C^* = k^* \times V_S / a$ where $*$ denotes P- or S-waves. Combining these formulae gives $f_C^* = (k^* \times V_S) \times (16 \times \Delta\sigma / (7 \times M_0))^{1/3}$. For the Pohang granite, $V_S = 3305\text{m s}^{-1}$ (Hofmann et al., 2019) or 3310m s^{-1} (Woo et al., 2019). Woo et al. (2019) determined $\Delta\sigma = 5.6\text{MPa}$ for the $M_W = 5.5$ event and assumed the same value for smaller events.

This theory can be applied, using $\Delta\sigma = 5.6\text{MPa}$ and $V_S = 3305\text{m s}^{-1}$, with $k_P = 0.38$ and $k_S = 0.26$ for sources that rupture at speed $V_R = 0.9 \times V_S$ (Kaneko and Shearer, 2014). Thus, for $M_W = 2.0$, $M_0 = 1.12 \times 10^{12}\text{N m}$, $f_{CP} = 28\text{Hz}$ and $f_{CS} = 19\text{Hz}$. For $M_W = 1.5$, $M_0 = 2.00 \times 10^{11}\text{N m}$, $f_{CP} = 50\text{Hz}$ and $f_{CS} = 34\text{Hz}$. For $M_W = 1.0$, $M_0 = 3.55 \times 10^{10}\text{N m}$, $f_{CP} = 89\text{Hz}$ and $f_{CS} = 61\text{Hz}$. For $M_W = 0.5$, $M_0 = 6.31 \times 10^9\text{N m}$, $f_{CP} = 159\text{Hz}$ and $f_{CS} = 109\text{Hz}$. For $M_W = 0.0$, $M_0 = 1.12 \times 10^9\text{N m}$, $f_{CP} = 283\text{Hz}$ and $f_{CS} = 193\text{Hz}$. Other studies propose higher k_P and k_S , for example Sato and Hirasawa (1973) reported $k_P = 0.42$ and $k_S = 0.29$ for $V_R = 0.9 \times V_S$. Higher values also arise for $V_R > 0.9 \times V_S$; for example, the Brune (1970) source model, which assumes instantaneous rupture, has $k_S = 0.37$. Furthermore, the aforementioned values are averaged over the focal sphere; Kaneko and Shearer (2014) reported that, for $V_R = 0.9 \times V_S$, k_P and k_S peak at 0.73 in some directions, which would indicate $f_{CP} = f_{CS} = 54\text{Hz}$ for $M_W = 2.0$. This analysis indicates the impact of the long sampling-interval for station PHA2 on the accuracy of magnitude determinations for $M_W < \sim 2.0$.

Furthermore, 'detective work' is needed to understand the magnitudes determined by Lee et al. (2019), Woo et al. (2019) and Lachenbruch et al. (2020). Thus, Lee et al. (2019) reported 98 events spanning November 2015–November 2017, including the $M_W = 5.5$ mainshock; for all these they reported M_L , for 46 events they also reported M_W . Woo et al. (2019) reported the same 98 M_L and 46 M_W determinations. They explained that for 40 events they determined M_L conventionally, synthesizing the response of a Wood-Anderson seismograph and applying the Sheen et al. (2018) regional M_L formula, listing these 40 'template events' (TEs) (excluding the mainshock) in their supplementary Table S2, 39 of them (including the mainshock) being included in the 98 catalogued. For the other 59 events, Woo et al. (2019) determined magnitudes by template matching (TM) seismograms from PHA2, these magnitudes being designated here as M_T . Peng and Zhao (2009) stated that TM is calibrated assuming one magnitude unit indicates a ten-fold S-wave amplitude-ratio. Woo et al. (2019) thus, effectively, used the formula $M_T = M_{LT} - \log_{10}(A_L/A_T)$ where M_{LT} is M_L for whichever TE was used to determine each M_T , and A_L/A_T the S-wave amplitude-ratio at PHA2 for the two events. The 98-event Woo et al. (2019) catalogue is thus a mix of M_T and true M_L values, all reported as M_L . Two of their 46 M_W values

were determined in the frequency-domain using seismograms from PHA2: S-wave spectra for the mainshock ($M_W=5.56$); P-wave spectra for the largest event during the stimulations, at 02:31:13 on April 15, 2017 (M_W 3.29). The other 44 (reported as M_W 0.58-2.72) were by time-domain integration of P-wave signals, after Tsuboi et al. (1995), again using PHA2 data.

Langenbruch et al. (2020) reported a 234-event catalogue spanning February 2016-November 2017. This includes the $M_W=5.5$ mainshock and 37 of the Woo et al. (2019) TEs, all with the same M_L values, plus their 59 M_T values and 137 ‘new’ events. For each of the latter 196 events, Langenbruch et al. (2020) reported M_T , which for the 59 events in common differed from the Woo et al. (2019) M_T values by ≤ 0.2 units. However, for the 04:58 event on August 13, 2017, for which Langenbruch et al. (2020) reported $M_T=-0.42$, well below the definitive $M_W=1.20$ (Hofmann et al., 2019), there is evidently a substantial discrepancy.

Langenbruch et al. (2020) stated that to ensure reliable b-values they used a uniform catalogue of M_L values, but this is clearly not so; they used a mix of 38 M_L and 196 M_T values. The accuracy of their M_L values is questionable because the Sheen et al. (2018) formula for M_L in Korea, which they used, was not calibrated for $M_L < 2.0$ and was based on few data for source-station distances ≤ 10 km, it being designed (to supersede M_K) for application to larger earthquakes at regional distances. Also, the determination of M_T , equating a ten-fold S-wave amplitude-ratio to one magnitude unit, is unsupported by theory, especially as the PHA2 data are bandwidth-limited (i.e., $f_N < \sim f_C$). Furthermore, for the August 2017 earthquake population, which was not bandwidth-limited (i.e., $f_N \gg f_C$) the ratio at MSS-01 is anyway ~ 20 (Fig. 2(b)) not 10. With this higher ratio, the Langenbruch et al. (2020) earthquake population is ‘compressed’ into a smaller M_T range, causing a higher b-value (~ 1.0 ; Fig. 1(b)) and reducing the predicted probabilities of $M_L \geq 5.0$ and ≥ 6.0 events to $\sim 0.3\%$ and $\sim 0.03\%$. The two Woo et al. (2019) frequency-domain M_W values are evidently reliable, being comparable with other results (e.g., Grigoli et al., 2018; Kim et al., 2018). However, their time-domain values utilised a technique that assumes broadband data (e.g., Tsuboi et al., 1995), and which, with $f_C > f_N$, can be expected to underestimate true M_W values by increasing margins as M_W decreases and f_C increases. Woo et al. (2019) used the $\sim 1:1$ relation between their M_W and M_T to validate both determinations; however, for the above-mentioned reasons, both might well diverge increasingly from ‘true’ magnitude values as the earthquakes become smaller. This underestimation is clear for the August 13, 2017, events: at 04:58, where Langenbruch et al. (2020) reported $M_T=-0.43$, well below the definitive $M_W=1.20$ (Hofmann et al., 2019); and at 21:42, where Woo et al. (2019) reported $M_W=1.21$ and $M_L=0.67$, well below the definitive $M_W=1.93$ (Hofmann et al., 2019).

The potential effect of miscalibration of M_T values, meaning ‘uncorrected’ values M_{TU} calculated using the formula $M_{TU}=M_{LT}-\log_{10}(A_L/A_T)$, may be estimated as follows. The ‘corrected’ value M_{TC} is intended to provide a true proxy for M_L below some threshold M_{LO} , with $M_{TC}=M_{LT}-K \times \log_{10}(A_L/A_T)$ and K a constant. It follows that $M_{TC}=(1-K) \times M_{LT}+K \times M_{TU}$. If $K=1/\log_{10}(20)$, consistent with Fig. 2(b), $b=1$ and Fig. 1(a) adjusts to Fig. 1(b), whereas if $K=0.64$ and $b=1.12$, as in Fig. 2(a), Fig. 1(a) adjusts to Fig. 1(c), the predicted probabilities of $M_L \geq 5.0$ and ≥ 6.0 events reducing to $\sim 0.1\%$ and $\sim 0.01\%$. Other adjustments are also possible, for example $b=2$ would arise from setting $K=0.36$, would yield M_T values for the August 13, 2017,

events of ~ 1.1 and ~ 1.5 , similar to the Hofmann et al. (2019) M_W values, and would reduce the predicted probabilities of $M_L \geq 5.0$ and ≥ 6.0 events to $\sim 0.0003\%$ and $\sim 0.000003\%$ (Fig. 1(d)). However, because Langenbruch et al. (2020) have not reported the S-wave amplitude-ratios at PHA2 that they used for their TM, nor which TE, and thus which M_{LT} value, was used to determine which M_T values, no definitive ‘correction’ is possible.

3 Conclusions

Langenbruch et al. (2020) are correct to note that, in principle, populations of small induced earthquakes can be extrapolated to determine probabilities of EGS projects causing events large enough to be destructive, to estimate the resulting costs. This methodology might usefully be adopted in future, possibly in association with regulatory guidelines or the arrangement of insurance. However, the mixed nature of the complex dataset of direct and proxy magnitude determinations for the Pohang earthquake population and the associated calibration problems, some resulting from the low Nyquist frequency of the PHA2 records relative to the corner frequencies of $M_W < \sim 2$ events, cast doubt on the low b-values determined by Langenbruch et al. (2020). The resulting high probabilities of destructive events ($\sim 5\%$ and $\sim 1\%$, respectively, for magnitudes ≥ 5.0 and ≥ 6.0) are thus also called into question; with higher b-values, these probabilities might be orders-of-magnitude lower. Aspects of the Pohang EGS project raise cause for concern (e.g., Lee et al., 2019); some of its personnel are indeed under investigation for prosecution for manslaughter. However, the criticism by Langenbruch et al. (2020) that they failed to recognise unusually low b-values and their potential consequences is inappropriate.

Acknowledgments

This work was supported by the European Commission Horizon 2020 research and innovation program under grant agreement No. 691728 (DESTRESS).

References

- Baraniuk, C., 2019. The mystery of unexplained earthquakes: from the UK to South Korea, seismic “detectives” are tracking the causes of anomalous tremors. BBC Future online, <https://www.bbc.com/future/article/20190708-the-mystery-of-unexplained-earthquakes>
- Brune, J. (1970). Tectonic stress and the spectra of seismic shear waves from earthquakes. *Journal of Geophysical Research*, 75, 4997–5009 (with 1971 correction: *Journal of Geophysical Research*, 76, 5002).
- Dempsey, D., Suckale, J., & Huang, Y. (2016). Collective properties of injection-induced earthquake sequences: 2. Spatiotemporal evolution and magnitude frequency distributions. *Journal of Geophysical Research, Solid Earth*, 121, 3638–3665.
- Ellsworth, W.L., Giardini, D., Townend, J., Ge, S.M., & Shimamoto, T. (2019). Triggering of the Pohang, Korea, earthquake (M_W 5.5) by Enhanced Geothermal System stimulation. *Seismological Research Letters*, 90, 1844–1858.

- 264 Eshelby, J.D. (1957). The determination of the elastic field of an ellipsoidal inclusion, and
265 related problems. *Proceedings of the Royal Society of London, Series A*, 241, 376–396.
- 266 Grigoli, F., Cesca, S., Rinaldi, A.P., Manconi, A., López-Comino, J.A., Clinton, J.F., Westaway,
267 R., Cauzzi, C., Dahm, T., & Wiemer, S. (2018). The November 2017 M_w 5.5 Pohang
268 earthquake: A possible case of induced seismicity in South Korea. *Science*, 360, 1003-
269 1006.
- 270 Hanks, T.C., & Kanamori, H. (1979). A moment magnitude scale. *Journal of Geophysical*
271 *Research*, 84, 2348–2350.
- 272 Hofmann, H., Zimmermann, G., Farkas, M., Huenges, E., Zang, A., Leonhardt, M., Kwiatak, G.,
273 Martinez-Garzon, P., Bohnhoff, M., Min, K.-B., Fokker, P., Westaway, R., Bethmann, F.,
274 Meier, P., Yoon, K.S., Choi, J.W., Lee, T.J., & Kim, K.Y. (2019). First field application
275 of cyclic soft stimulation at the Pohang Enhanced Geothermal System site in Korea.
276 *Geophysical Journal International*, 217, 926–949.
- 277 Kaneko, Y., & Shearer, P.M. (2014). Seismic source spectra and estimated stress drop derived
278 from cohesive-zone models of circular subshear rupture. *Geophysical Journal*
279 *International*, 197, 1002–1015.
- 280 Kim, K.-H., Ree, J.-H., Kim, Y., Kim, S., Kang, S.Y., & Seo, W. 2018. Assessing whether the
281 2017 M_w 5.4 Pohang earthquake in South Korea was an induced event. *Science*, 360,
282 1007-1009.
- 283 Langenbruch, C., Ellsworth, W.L., Woo, J.-U., & Wald, D.J. (2020). Value at induced risk:
284 injection-induced seismic risk from low-probability, high-impact events. *Geophysical*
285 *Research Letters*, 47, e2019GL085878, 12 pp., <https://doi.org/10.1029/2019GL085878>
- 286 Lee, K.-K., Yeo, I.-W., Lee, J.-Y., Kang, T.-S., Rhie, J., Sheen, D.-H., Chang, C., Son, M., Cho,
287 I.-K., Oh, S., Pyun, S., Kim, S., Ge, S., Ellsworth, W.L., Giardini, D., Townend, J., &
288 Shimamoto, T. (2019). Summary report of the Korean Government Commission on
289 relations between the 2017 Pohang earthquake and the EGS project. Geological Society
290 of Korea and Korean Government Commission on the Cause of the Pohang Earthquake,
291 Seoul, Republic of Korea, 205 pp.
292 [http://www.gskorea.or.kr/custom/27/data/Summary_Report_on_Pohang_Earthquake_Ma](http://www.gskorea.or.kr/custom/27/data/Summary_Report_on_Pohang_Earthquake_March_20_2019.pdf)
293 [rch_20_2019.pdf](http://www.gskorea.or.kr/custom/27/data/Summary_Report_on_Pohang_Earthquake_March_20_2019.pdf)
- 294 Lee, T.J., Song, Y.H., Yoon, W.S., Kim, K.-Y., Jeon, J.G., Min, K.-B., & Cho, Y.-H., 2011. The
295 first Enhanced Geothermal System Project in Korea. Proceedings of the 9th Asian
296 Geothermal Symposium, November 7-9, 2011. [https://www.geothermal-](https://www.geothermal-energy.org/pdf/IGAstandard/Asian/2011/23_Tae_Jong_Lee.pdf)
297 [energy.org/pdf/IGAstandard/Asian/2011/23_Tae_Jong_Lee.pdf](https://www.geothermal-energy.org/pdf/IGAstandard/Asian/2011/23_Tae_Jong_Lee.pdf)
- 298 Madariaga, R. (1976). Dynamics of an expanding circular fault. *Bulletin of the Seismological*
299 *Society of America*, 66, 639–666.
- 300 Madariaga, R., & Ruiz, S. (2016). Earthquake dynamics on circular faults: A review 1970–2015.
301 *Journal of Seismology*, 20, 1235–1252.
- 302 Peng, Z.G., & Zhao, P. (2009). Migration of early aftershocks following the 2004 Parkfield
303 earthquake. *Nature Geoscience*, 2, 877-881.

- Sato, T., & Hirasawa, T. (1973). Body wave spectra from propagating shear cracks. *Journal of Physics of the Earth*, 21, 415–431.
- Smith, W.D. (1981). The b-value as an earthquake precursor. *Nature*, 289, 136–139.
- Tsuboi, S., Abe, K., Takano, K., & Yamanaka, Y. (1995). Rapid determination of M_w from broadband P waveforms. *Bulletin of the Seismological Society of America*, 85, 606–613.
- Westaway, R., & Burnside, N.M. (2019). Fault ‘corrosion’ by fluid injection: potential cause of the November 2017 M_w 5.5 Korean earthquake. *Geofluids*, 2019, 1280721, 23 pp., <https://doi.org/10.1155/2019/1280721>
- Westaway, R., Burnside, N.M., & Banks, D. (2020). Hydrochemistry of produced water from the Pohang EGS project site, Korea: Implications for water-rock reactions and associated changes to the state of stress accompanying hydraulic fracturing of granite. Proceedings, World Geothermal Congress 2020, Reykjavik, Iceland, April 26 - May 2, 2020. Paper 15037, 12 pp. <https://pangea.stanford.edu/ERE/db/WGC/papers/WGC/2020/15037.pdf>
- Westaway, R., & Younger, P.L. (2014). Quantification of potential macroseismic effects of the induced seismicity that might result from hydraulic fracturing for shale gas exploitation in the UK. *Quarterly Journal of Engineering Geology and Hydrogeology*, 47, 333–350.
- Woo, J.-U., Kim, M., Sheen, D.-H., Kang, T.-S., Rhie, J., Grigoli, F., Ellsworth, W.L., & Giardini, D., 2019. An in-depth seismological analysis revealing a causal link between the 2017 M_w 5.5 Pohang earthquake and EGS project. *Journal of Geophysical Research, Solid Earth*, 124, 13,060–13,078.
- Yoon, K.-S., Jeon, J.-S., Hong, H.-K., Kim, H.-G., Hakan, A., Park, J.-H., & Yoon, W.-S. (2015). Deep Drilling Experience for Pohang Enhanced Geothermal Project in Korea. Proceedings, World Geothermal Congress 2015, Melbourne, Australia, April 19-25, 2015. <https://pangea.stanford.edu/ERE/db/WGC/papers/WGC/2015/06034.pdf>
- Zhang, M., & Wen, L. (2015). An effective method for small event detection: Match and locate (M&L). *Geophysical Journal International*, 200, 1523–1537.